Two-dimensional Intensity Distribution and Connectivity in Ultraviolet Ad-Hoc Network

Hong Qi, Difan Zou, Chen Gong, and Zhengyuan Xu
Key Laboratory of Wireless-Optical Communications, Chinese Academy of Sciences
University of Science and Technology of China
Hefei, Anhui 230027, China
Email: {hongqi,knowzou}@mail.ustc.edu.cn, {cgong821,xuzy}@ustc.edu.cn.

***Abstract*—Consider directional antenna array in an ultraviolet (UV) scattering communication Ad-Hoc network. To efficiently obtain the link gain coverage of single antenna, we propose an algorithm based on one-dimensional (1D) numerical integration and an off-line data library. We also analyze the two-dimensional (2D) scattering intensity distribution, where numerical results show that the path loss profile can be well fitted by elliptic models. In addition, assume that the node distribution in Ad-Hoc network obeys Poisson point process (PPP). For both directional antenna array and omnidirectional antenna, adopting ellipses and circles to represent the coverage of nodes, we investigate the minimum power such that the network still keeps connected. Simulation results show that employing directional antenna array can effectively reduce the minimum power that guarantees coverage.**

I. Introduction

Non-line-of-sight (NLOS) ultraviolet (UV) communication serves as an alternative transmission solution when the radio-frequency (RF) is prohibited, not only due to the scattering event that can guarantee NLOS link, but also due to extremely weak solar background radiation [1].

Recently, NLOS UV scattering communication has been extensively investigated in terms of channel modeling [2], [3], signal characterization and performance analysis [4]–[6]. For UV communication networks, such as broadcasting and Ad-Hoc networks, the connectivity has been studied in [7], [8]. However, specific shape of the node coverage area and the related network performance have not be characterized. The above two fundamental characteristics are crucial to the analysis and design of UV communication networks.

Traditionally, the link gain of scattering communication channel can be obtained based on Monte Carlo method [9], [10], theoretical analysis [11]–[14] and experimental results [15], [16]. However, high computational cost of the Monte Carlo method may impede the real-time computation of link gain. Therefore, analytical or semi-analytical methods need to be explored to obtain the intensity distribution efficiently. However, for a large field-of-view (FOV) of each receiver, the approximation on the scattering common volume [11], [13] does not well approximate, and thus a more accurate approach is needed.

This work was supported by National Key Research and Development Program of China (Grant No. 2018YFB1801904), Key Program of National Natural Science Foundation of China (Grant No. 61631018) and Key Research Program of Frontier Sciences of CAS (Grant No. QYZDY-SSW-JSC003).

On the other hand, UV scattering communication is typically applied to emergency and military communication, which shows significant potential in an Ad-Hoc network [17]. A primary challenge is the coverage issue and the related energy consumption [18]–[20], which can be improved by the antenna structure design.

In this paper, we consider a laser source, and propose an analytical approximation to the link gain as a function with respect to the elevation angle and the receiver's 2D position. Based on the proposed algorithm, the two-dimensional scattering intensity distribution pattern is discussed, and it is observed that the elliptical model can well fit the contour. Then, we assume an Ad-Hoc network satisfying Poisson point process (PPP) [21], where the link gain coverage of a node with directional antenna array can be fitted by an ellipse, whose shape is directly related to the source elevation angle and divergence angle. Through a distributed sensing algorithm, we can investigate the relationship between the mean power and antenna parameters.

II. Two-dimensional intensity distribution of scattering

A. Scattering Model with Efficient Link Gain Representation

Consider the atmospheric UV communication with both scattering and absorption. In general, Rayleigh scattering coefficient k_s^{ray}, Mie scattering coefficient k_s^{mie}, and absorption coefficient k_a are adopted to characterize the scattering and absorption intensities. Moreover, let $k_s = k_s^{ray} + k_s^{mie}$ and $k_t = k_a + k_s$ denote the scattering coefficient and total extinction coefficient, respectively.

In order to determine the achievable communication area at the transmitting end, it is necessary to analyze the contour of such two-dimensional (2D) intensity distribution to determine the achievable communication area for different user positions. The geometric configuration of the transmission path is shown in Figure 1. The transmitter position is set to be $(0, 0, 0)$. Let $(x, y, 0)$ denote the receiver position, l and l' denote the distance from scattering point to the transmitter and receiver, respectively. Let α be the elevation angle between the laser axis and Y-axis, θ be the scattering angle between the light direction and the line from scattering point to the receiver, $\Omega(l)$ be the solid angle of Rx at each scattering point $(0, l\cos\alpha, l\sin\alpha)$, and A_r be the area of receiver aperture.

978-1-7281-5089-5/20/$31.00 ©2020 IEEE

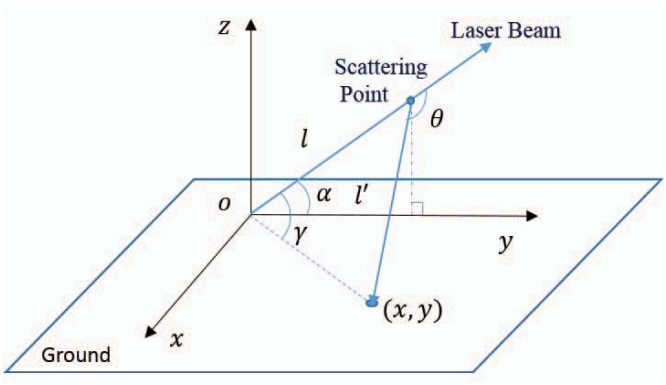

Fig. 1. The geometric description of the UV scattering radiation.

Letting E_t be the intensity of transmitted UV signal, the power of signal scattered at $(0, l\cos\alpha, l\sin\alpha)$ and detected by the receiver is given by

$$\delta E_r(l) = E_t P[\mu(l)]\,\Omega(l) e^{-k_a(l+l')} e^{-k_s l'}\delta l, \tag{1}$$

where $\mu(l) = \cos\theta_s$ is a function of x, y, α, and l, given by $\mu(x,y,\alpha,l) = \frac{y\cos\alpha - l}{l'}$; and $\Omega(l)$ denotes the solid angle from receiving area to scattering point $(0, l\cos\alpha, l\sin\alpha)$, given by $\Omega(x,y,\alpha,l) = \frac{A_r}{l'^2}\frac{l\sin\alpha}{l'}$. Let $P(\mu)$ denote the scattering phase function, which could be obtained from [9]. In the atmosphere, free distance l satisfies exponential distribution $f(l) = k_s e^{-k_s l}$.Then, the total received power at $(x,y,0)$ is given by

$$\begin{aligned} E_r &= \int_0^\infty E_t P[\mu(l)]\,\Omega(l) e^{-k_a(l+l')} e^{-k_s l'} k_s e^{-k_s l} dl \\ &= \int_0^\infty E_t P[\mu(l)]\,\Omega(l) k_s e^{-(k_a+k_s)(l+l')}\mathrm{d}l. \end{aligned} \tag{2}$$

Hence, link gain function $L_g(x,y,\alpha)$ is given by

$$L_g(x,y,\alpha) = \int_0^\infty P(\mu)\,\Omega(l) k_s e^{-(k_a+k_s)(l+l')}\mathrm{d}l. \tag{3}$$

The one-dimensional (1D) numerical integration can reduce the simulation time dramatically compared with the Monte Carlo method [9], [10]. However, it still requires high computational complexity. To address this issue, we aim to investigate whether it can be represented by variables in a lower-dimensional space. Motivated by this, we provide the following result.

Theorem 1. *If the link gain is calculated in accordance with (3), we have the following,*

$$L_g(x,y,\alpha) = \frac{L_g(0,\sqrt{x^2+y^2},\beta)\sin\alpha}{\sin\beta}, \tag{4}$$

where $\cos\beta = \cos\gamma\cos\alpha$ *and* $\tan\gamma = \frac{x}{y}$.

Proof. For the link gain $L_g(x,y,\alpha)$, we have

$$\begin{aligned} l'^2 &= x^2 + (y - l\cos\alpha)^2 + l^2\sin^2\alpha \\ &= x^2 + y^2 + l^2 - 2yl\cos\alpha \\ &= y'^2 + l^2 - 2y' l\cos\alpha', \end{aligned} \tag{5}$$

where $y' = \sqrt{x^2+y^2}$ and $\cos\alpha' = \frac{y}{y'}\cos\alpha = \cos\alpha\cos\gamma$. This equation implies that $l'(x,y,\alpha,l) = l'(0,y',\alpha',l)$. For the cosine of scattering angle, we have

$$\mu(x,y,\alpha,l) = \cos\theta_s = \frac{y\cos\alpha - l}{l'} = \frac{y'\cos\alpha' - l}{l'}, \tag{6}$$

which implies that $\mu(x,y,\alpha,l) = \mu(0,y',\alpha',l)$. As for the solid angle $\Omega(x,y,\alpha,l)$, we have

$$\Omega(x,y,\alpha,l) = \frac{A_r l\sin\beta}{l'^3}\frac{\sin\alpha}{\sin\beta} = \Omega(0,y',\alpha',l)\frac{\sin\alpha}{\sin\beta}. \tag{7}$$

Substituting the above results into equation (8), we have

$$\begin{aligned} L_g(x,y,\alpha) &= \int_0^\infty P(\mu)\,\Omega(l) k_s e^{-(k_a+k_s)(l+l')}\mathrm{d}l \\ &= \int_0^\infty P(\mu')\,\Omega'(l)\frac{\sin\alpha}{\sin\beta} k_s e^{-(k_a+k_s)(l+l')}\mathrm{d}l \\ &= L_g(0,y',\alpha'), \end{aligned} \tag{8}$$

where $\mu' \triangleq \mu(0,y',\alpha',l)$ and $\Omega'(l) \triangleq \Omega(0,y',\alpha',l)$. □

Thus, a 2D library $\boldsymbol{L} \triangleq \{L(0,r_i,\alpha_i), r_i \in \boldsymbol{r}, \alpha_i \in \boldsymbol{\alpha}\}$ is constructed, where $\boldsymbol{r}$ denotes the set of different communication ranges when the receiver locates at Y-axis, and $\boldsymbol{\alpha}$ denotes the set of different elevation angles (typically we set $\boldsymbol{r} = [0:1:1000]$ and $\boldsymbol{\alpha} = \pi \times [0.005:0.005:1]$). Then, the link gain $L_g(x,y,\alpha)$ could be calculated by obtaining $L_g(0,(x^2+y^2)^{1/2},\beta)$ from library $\boldsymbol{L}$, and multiplying by $\sin\alpha/\sin\beta$, where $\tan\beta = x/y$. For a special case that $\alpha = 90°$, we have $\beta = 90°$ and $L_g(x,y,90°) = L_g(0,\sqrt{(x^2+y^2)},90°)$, which implies a circular shape for the contour of 2D scattering intensity distribution.

Assume uniform pattern for the beam produced by the light source. In order to calculate the link gain for a wide-beam source, we generate multiple narrow beams with uniformly distributed random direction, and average the corresponding link gains. Assuming that the center direction of light is $(0,\cos\alpha,\sin\alpha)$, the full divergence angle is ϕ_d. Let $\boldsymbol{\zeta'} = (\zeta'_x,\zeta'_y,\zeta'_z)$ denote the random emitting direction. It can be generated according to the coordinate transformation, specified by

$$\begin{aligned} \zeta'_x &= \sin\theta'\sin\phi', \\ \zeta'_y &= -\sin\theta'\cos\phi'\sin\alpha + \cos\theta'\cos\alpha, \\ \zeta'_z &= \sin\theta'\cos\phi'\cos\alpha + \cos\theta'\sin\alpha, \end{aligned} \tag{9}$$

where θ' and ϕ' are random angles generated by $\theta' = \arccos\left[1 - \xi(1-\cos\frac{\phi_d}{2})\right]$ and $\phi' = 2\pi\xi$, where ξ denotes a uniformly distributed random variable between zero and one.

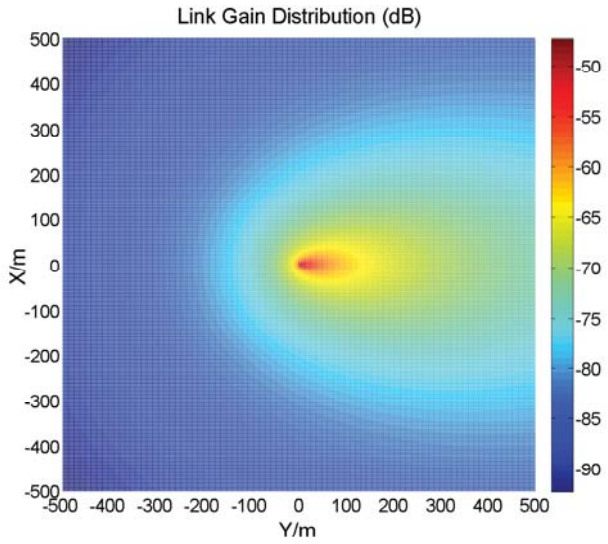

Fig. 2. The 2D radiation distribution for laser source with elevation angle $\alpha = 30°$.

Let $L'_g(x, y, \boldsymbol{\zeta'})$ denote the link gain for the laser with normalized direction $\boldsymbol{\zeta'}$, which can be mapped into standard form $L_g(x', y', \alpha')$ via coordinate transformation, given by

$$\begin{aligned} x' &= \frac{\zeta'_y}{\sqrt{1-\zeta'^2_z}}x - \frac{\zeta'_x}{\sqrt{1-\zeta^2_z}}y, \\ y' &= \frac{\zeta'_x}{\sqrt{1-\zeta'^2_z}}x + \frac{\zeta'_y}{\sqrt{1-\zeta^2_z}}y, \\ \alpha' &= \arccos(\zeta'_z). \end{aligned} \tag{10}$$

Hence, for each laser beam, we can obtain the corresponding link gain based on library $\boldsymbol{L}$. By averaging the link gains of sufficiently large number of randomly generated narrow beams, we have the following link gain with a wide-beam source,

$$L_g^{WB}(x, y, \alpha, \phi_d) = \frac{1}{N}\sum_{k=1}^{N} L'_g(x, y, \boldsymbol{\zeta'_k}). \tag{11}$$

B. Coverage with Different Elevation Angles

Assuming that the receivers are distributed in a squared area, we obtain a two-dimensional scattering intensity distribution according to the above formulas. Specifically, we simulate 500×500 link gains in area $[-500, 500]m \times [-500, 500]m$, and the 2D radiation distribution for the laser source with elevation angle $\alpha = 30°$ is shown in Figure 2.

It can be observed that the contour can be fitted by an ellipse. Motivated by this, we extract the contour coordinates, denoted as $(\boldsymbol{X}, \boldsymbol{Y}) = \{(x_i, y_i), i = 1, 2, \ldots, M\}$. Then, we perform fitting based on the following elliptic function

$$\frac{(x - x_0)^2}{a^2} + \frac{(y - y_0)^2}{b^2} = 1, \tag{12}$$

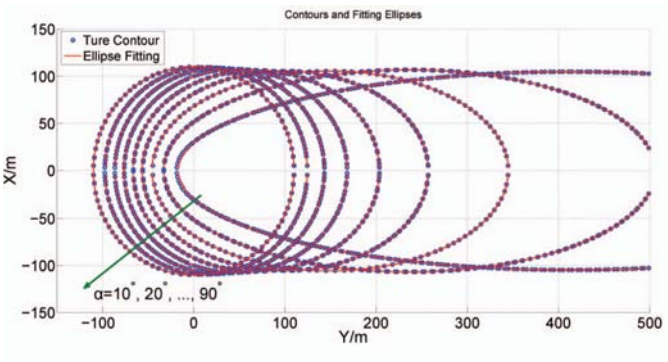

Fig. 3. The contours and fitting ellipses of 2D radiation distribution for the laser source with elevation angle from $10°$ to $90°$ ($L_g = 10^{-7}$).

where $x_0 = 0$ due to the fact $L_g(x, y, \alpha) = L_g(-x, y, \alpha)$. The ellipse parameters y_0, a, b can be obtained based on the following least squares criterion

$$\min_{y_0,a,b} \sum_{i=1}^{M} \left[a^2 \left(1 - \frac{y_0^2}{b^2} + \frac{2y_0}{b^2}y_i - \frac{y_i^2}{b^2} \right) - x_i^2 \right]^2. \tag{13}$$

Letting $\boldsymbol{k} = \left[a(1 - \frac{y_0^2}{b^2}), \frac{2a^2 y_0}{b^2}, -\frac{a^2}{b^2} \right]^T$ denote the parameter vector, the optimal fitting solution is given by

$$\boldsymbol{k} = (\boldsymbol{Y}_{M,3}^T \boldsymbol{Y}_{M,3})^{-1} \boldsymbol{Y}_{M,3}^T \boldsymbol{x}_2, \tag{14}$$

where $\boldsymbol{Y}_{M,3}$ is a 3-order Vandermonde matrix of parameters $\{y_1, y_2, \ldots, y_M\}$ and $\boldsymbol{x}_2 \triangleq [x_1^2, x_2^2, \ldots, x_M^2]^T$.

Figure 3 shows the contours and the corresponding fitting ellipses for elevation angle from $10°$ to $90°$, where the link threshold is set to be 10^{-7}. It can be seen that the ellipse curve can well model the contour of 2D radiation distribution. As the elevation angle increases, the coverage area decreases and the contour becomes a circle when $\alpha = 90°$.

C. Coverage for Different Divergence Angles

We investigate the relationship between the ellipse characteristics and divergence angle ϕ_d. Figure 4 shows that the contour size increases with respect to the divergence angle, but not sensitive to it. Moreover, it can be observed that the left endpoint of the fitting ellipses basically remains the same but the right endpoint only changes from $(0, 350)$ to $(0, 400)$.

III. Power Minimization for Ad-Hoc Network Connection

A. Transmitter Configuration and Receiver Distribution

Assume that the transmitter employs a directional antenna array [22], [23], where each array element covers an area of ellipse shape, as shown in Figure 5. The design of antenna array involves the number N of directional antennas and elevation angle α of a single antenna. The divergence angle of each antenna element can be determined by the criterion that $\phi_d = 360°/N$.

To characterize the link coverage in the Ad-Hoc network, we fit path loss $1/L_g$ and distance x_1 from the emitter to the

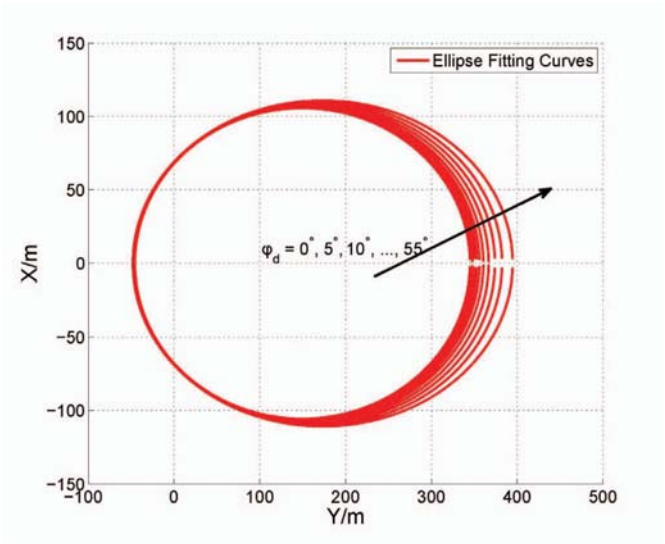

Fig. 4. The ellipse fitting of the contour of 2D radiation distribution for the case $(\alpha, \phi_d) = (30°, 0° - 55°)$ $(L_g = 10^{-7})$.

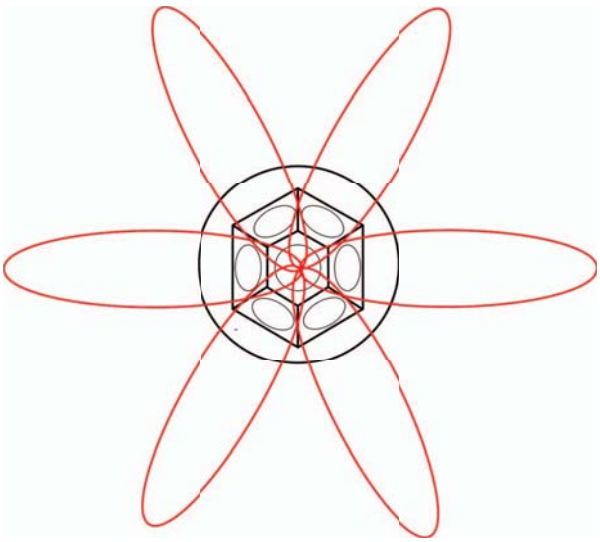

Fig. 5. The coverage of a directional UV antenna array.

ellipse center using the long axis length a, as shown in Table I. Moreover, assume that the node distribution in the Ad-Hoc network satisfies Poisson point process (PPP). For area S, the number of node M satisfies Poisson distribution with mean λS, given by,

$$P\left(M = m\right) = \frac{\left(\lambda S\right)^m}{m!} e^{-(\lambda S)}, \tag{15}$$

where λ is the node intensity of PPP.

Considering two nodes A and B, we need to investigate whether node A can communicate to node B, as shown in Figure 6. Assume that A is the origin pointing direction θ, and can sense the direction β of B. Thus, the angle from the transmitting direction is $\gamma = \theta - \beta$. According to the coordinate

TABLE I
FIT OF TRANSMISSION AND ELLIPSE PARAMETERS

α	$1/L_g$	$x_1(m)$	$b(m)$
10°	$6.7a^2 + 954.9a + 6801$	$0.987a + 0.950$	$a \sin 10°$
20°	$19.3a^2 + 2058a + 20780$	$0.879a + 2.980$	$a \sin 20°$
30°	$36.9a^2 + 2882a + 45220$	$0.735a + 4.774$	$a \sin 30°$
40°	$58.4a^2 + 2995a + 89750$	$0.583a + 5.973$	$a \sin 40°$
50°	$182.19a^2 + 2052a + 167900$	$0.439a + 6.421$	$a \sin 50°$
60°	$106.7a^2 - 119.2a + 293200$	$0.310a + 6.001$	$a \sin 60°$
70°	$130.2a^2 - 3577a + 481600$	$0.196a + 4.799$	$a \sin 70°$
80°	$1151.3a^2 - 8182a + 744400$	$0.094a + 2.784$	$a \sin 80°$
90°	$168.4a^2 + 13750a + 1096000$	0	a

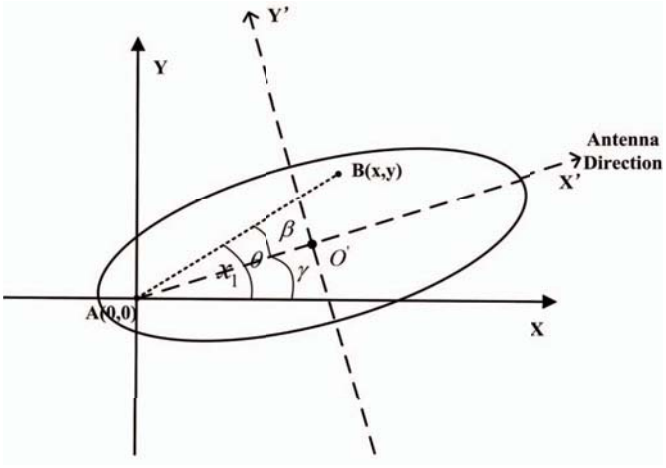

Fig. 6. The geometric model for the transmission.

transformation matrix (16), if B is in the ellipse, the following conditions must be satisfied,

$$\begin{bmatrix} x' \\ y' \end{bmatrix} = \begin{bmatrix} \cos\gamma & \sin\gamma \\ -\sin\gamma & \cos\gamma \end{bmatrix} \begin{bmatrix} x \\ y \end{bmatrix} - \begin{bmatrix} x_1 \\ 0 \end{bmatrix}, \tag{16}$$

$$\frac{x_B'^2}{a^2} + \frac{y_B'^2}{b^2} \leq 1, \tag{17}$$

where $b = a \sin\alpha$. Based on the relative positions of A, B, we can calculate the path loss between A and B.

Next, since each photon carries energy hc/λ , the received number of signal photons per second is $P_r \eta_f \eta_r \lambda/(hc)$, where $\eta_f = 0.1$ is the UV optical filter efficiency, $\eta_r = 0.2$ is the detector quantum efficiency, and $\lambda = 266nm$ is wavelength [11]. The maximum solar background radiation is approximately 5×10^4 counts per second in ultraviolet band [24]. Thus by calculation, setting the minimum receiving electric power of the receiver $P^r_{\min} = 10^{-11}W$, the condition that node i $(1 \leq i \leq m)$ can communicate to the node j $(1 \leq j \leq m)$ is given as follows,

$$P^t_{ij} \cdot L_g \geq P^r_{\min}. \tag{18}$$

For the network, we use graphs to show whether the node pairs are connected. Then, the mean power is $\frac{1}{m} \sum_{1 \leq i \leq m} \sum_{1 \leq j \leq m} P^t_{ij}$.

B. Power Allocation Algorithm

We employ the directional transmission antenna array and receiving antenna array [25], such that each node can sense the incoming angle and adjust the transmission direction pointing to the nearest node.

Assume that each node increases the transmission power for each antenna until the network becomes connected, and define this minimum sensing power among all nodes that can make the network connected as P^{Prec}. Then, the antennas that do not communicate can be turned off provided that the network still keeps connected, and we can obtain power $P_{Dire}^{Link} = \frac{1}{m}\sum_{1\le i\le m}\sum_{1\le j\le m} P_{ij}^{t}$.

Based on the connected network, all nodes can communicate to each other. For the set of m nodes, denoted as $\boldsymbol{V}$, randomly select a node, denoted as set $\boldsymbol{U}$. Choose nodes (u, v) with the minimum power, where node u belongs to set $\boldsymbol{U}$ and node v belongs to set $\boldsymbol{V}-\boldsymbol{U}$, add the node v to the set $\boldsymbol{U}$, and record the corresponding power of the connected edge as P_v. Repeat the above process until set $\boldsymbol{U}$ contains m nodes. By using Prim greedy algorithm, we can obtain the spanning tree with the minimum (MST) of power sides for the connected graph, and the corresponding sum power is $\sum_{2\le v\le m} P_v^t$. Therefore, for different antenna structures, we can get the mean via averaging such sum power, i.e., $P_{Dire}^{MST} = \frac{1}{m}\sum_{2\le v\le m} P_v^{Dire}$ and $P_{Omni}^{MST} = \frac{1}{m}\sum_{2\le v\le m} P_v^{Omni}$.

C. Simulation Results

The simulations parameters are shown in Table II. Examples on the network connectivity and the spanning tree corresponding to omnidirectional and directional antenna structures are shown in Figure 7 and Figure 8, respectively.

TABLE II
KEY PARAMETERS OF SIMULATION

Symbol	Physical meaning	Value/unit
S	Simulation area size	$1km^2$
λ	Node density	$40/km^2$
N	Number of direction antenna arrays	6
α	Directional antenna elevation angle	30°
N_0	Single case simulation times	20
$P_{\min}^{r}$	Minimum receiving power	$10^{-11}W$

Assume that λ varies from 10 to 100. The mean transmission power is shown in Figure 9. It can be seen that the directional antenna array can effectively reduce the mean power for low node intensity. The mean transmission power with respect to the number of antennas is shown Figure 10. It is also seen that the power is not sensitive to the number of antennas, since more antennas imply a wider communication angle but lower power per antenna.

IV. CONCLUSIONS

In this work, we have proposed an algorithm for efficiently representing the path loss of NLOS communication, which shows that the coverage contour is approximately elliptical. The results are applied to Ad-Hoc network and compared with the omnidirectional antenna. Based on the mean power of each node, it is shown that directional antenna array outperforms omnidirectional antenna for Ad-Hoc networks. Future work lies in antenna parameter optimization for layered Ad-Hoc networks.

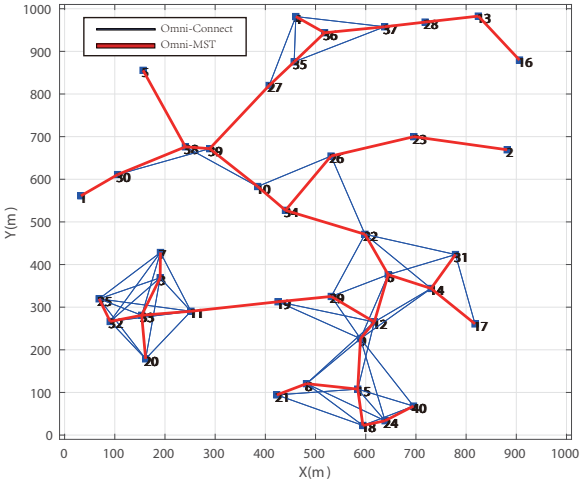

Fig. 7. Omnidirectional antenna network from the proposed approach and MST.

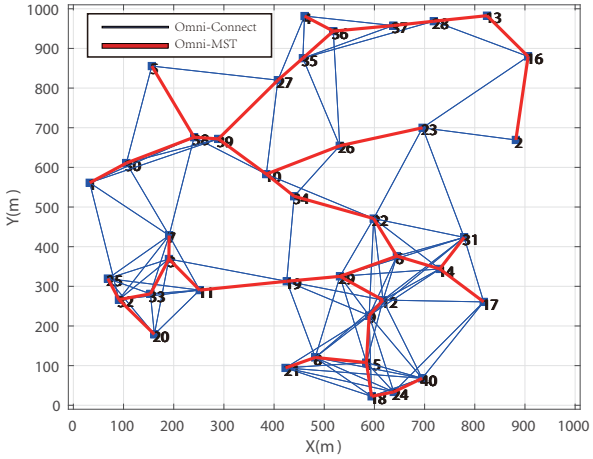

Fig. 8. Directional antenna array network from the proposed approach and MST.

REFERENCES

[1] Z. Xu and B. M. Sadler, "Ultraviolet communications: potential and state-of-the-art," *IEEE Communications Magazine*, vol. 46, no. 5, pp. 67–73, May. 2008.

[2] R. J. Drost, T. J. Moore, and B. M. Sadler, "Ultraviolet scattering propagation modeling: analysis of path loss versus range," *Journal of the Optical Society of America A*, vol. 30, no. 11, pp. 2259–2265, Sept. 2013.

[3] G. Chen, Z. Xu, H. Ding, and B. M. Sadler, "Path loss modeling and performance trade-off study for short-range non-line-of-sight ultraviolet communications," *Optics Express*, vol. 17, no. 5, pp. 3929–3940, 2009.

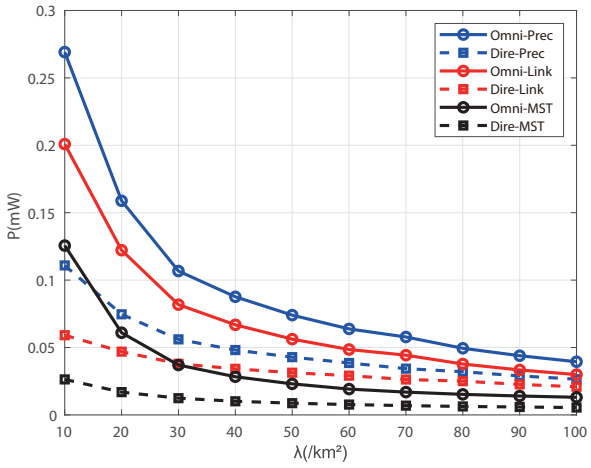

Fig. 9. The mean transmission power and node density for different antenna structures.

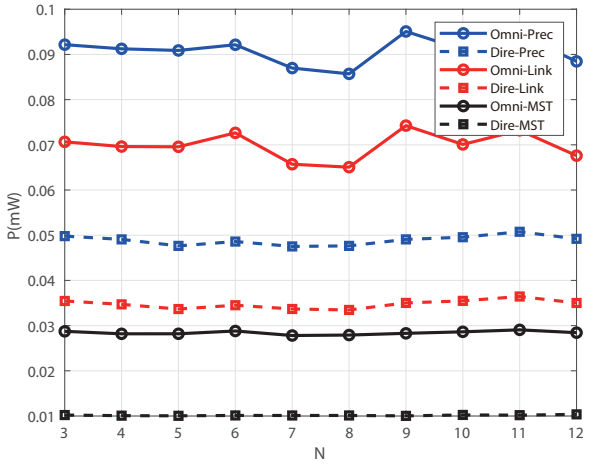

Fig. 10. The mean transmission power with respect to the number of antennas.

[4] Q. He, Z. Xu, and B. M. Sadler, "Performance of short-range non-line-of-sight led-based ultraviolet communication receivers," *Optics Express*, vol. 18, no. 12, pp. 12 226–12 238, 2010.

[5] R. J. Drost, B. M. Sadler, and G. Chen, "Dead time effects in non-line-of-sight ultraviolet communications," *Optics Express*, vol. 23, no. 12, pp. 15 748–15 761, 2015.

[6] C. Gong and Z. Xu, "Non-line of sight optical wireless relaying with the photon counting receiver: A count-and-forward protocol," *IEEE Transactions on Wireless Communications*, vol. 14, no. 1, pp. 376–388, Jan. 2015.

[7] L. Wang, Y. Li, and Z. Xu, "On connectivity of wireless ultraviolet networks," *Journal of the Optical Society of America A*, vol. 28, no. 10, pp. 1970–1978, Oct. 2011.

[8] A. Vavoulas, H. G. Sandalidis, and D. Varoutas, "Connectivity issues for ultraviolet uv-c networks," *IEEE Journal of Optical Communications and Networking*, vol. 3, no. 3, pp. 199–205, Mar. 2011.

[9] H. Ding, G. Chen, A. K. Majumdar, B. M. Sadler, and Z. Xu, "Modeling of non-line-of-sight ultraviolet scattering channels for communication," *IEEE Journal on Selected Areas in Communications*, vol. 27, no. 9, pp. 1535–1544, Sept. 2009.

[10] C. Xu, H. Zhang, and J. Cheng, "Effects of haze particles and fog droplets on nlos ultraviolet communication channels," *Optics Express*, vol. 23, no. 18, pp. 23 259–23 269, 2015.

[11] Z. Xu, H. Ding, B. M. Sadler, and G. Chen, "Analytical performance study of solar blind non-line-of-sight ultraviolet short-range communication links," *Optics Letters*, vol. 33, no. 16, pp. 1860–1862, 2008.

[12] L. Wang, Z. Xu, and B. M. Sadler, "Non-line-of-sight ultraviolet link loss in noncoplanar geometry," *Optics Letters*, vol. 35, no. 8, pp. 199–205, Aug. 2010.

[13] Y. Zuo, H. Xiao, J. Wu, Y. Li, and J. Lin, "Closed-form path loss model of non-line-of-sight ultraviolet single-scatter propagation," *Optics Letters*, vol. 38, no. 12, pp. 2116–2118, Jun. 2013.

[14] Y. Sun and Y. Zhan, "Closed-form impulse response model of non-line-of-sight single-scatter propagation," *Journal of the Optical Society of America A*, vol. 33, no. 4, pp. 752–757, Apr. 2016.

[15] L. Liao, Z. Li, T. Lang, and G. Chen, "UV LED array based NLOS UV turbulence channel modeling and experimental verification," *Optics Express*, vol. 23, no. 17, pp. 21 825–21 835, Aug. 2015.

[16] N. Raptis, E. Pikasis, and D. Syvridis, "Power losses in diffuse ultraviolet optical communications channels," *Optics Letters*, vol. 41, no. 18, pp. 4421–4424, Sept. 2016.

[17] Y. Li, L. Wang, Z. Xu, and S. V. Krishnamurthy, "Neighbor discovery for ultraviolet ad hoc networks," *IEEE Journal on Selected Areas in Communications*, vol. 29, no. 10, pp. 2002–2011, Oct. 2011.

[18] V. Kanakaris, D. Ndzi, and D. Azzi, "Ad-hoc networks energy consumption: a review of the ad-hoc routing protocols," *Journal of Engineering Science and Technology Review*, vol. 3, no. 1, pp. 162–167, 2010.

[19] F. Pianegiani, M. Hu, A. Boni, and D. Petri, "Energy-efficient signal classification in ad hoc wireless sensor networks," *IEEE Transactions on Instrumentation and Measurement*, vol. 57, no. 1, pp. 190–196, Jan. 2007.

[20] L. Gruenwald, M. Javed, and M. Gu, "Energy-efficient data broadcasting in mobile ad-hoc networks," in *Proceedings International Database Engineering and Applications Symposium*. IEEE, 2002.

[21] R. K. Ganti and M. Haenggi, "Spatial and temporal correlation of the interference in aloha ad hoc networks," *IEEE Communications Letters*, vol. 13, no. 9, pp. 631–633, Sept. 2009.

[22] A. Burton, H. Le Minh, Z. Ghassemlooy, S. Rajbhandari, and P. A. Haigh, "Smart receiver for visible light communications: Design and analysis," in *2012 8th International Symposium on Communication Systems, Networks & Digital Signal Processing*. IEEE, 2012.

[23] A. Burton, Z. Ghassemlooy, S. Rajbhandari, and S.-K. Liaw, "Design and analysis of an angular-segmented full-mobility visible light communications receiver," *Transactions on Emerging Telecommunications Technologies*, vol. 25, no. 6, pp. 591–599, 2014.

[24] G. Wang, K. Wang, C. Gong, D. Zou, Z. Jiang, and Z. Xu, "A 1mbps real-time nlos uv scattering communication system with receiver diversity over 1km," *IEEE Photonics Journal*, vol. 10, no. 2, pp. 1–13, Apr. 2018.

[25] H. Qi, C. Gong, and Z. Xu, "Omnidirectional antenna array-based transmitter direction sensing in ultra-violet ad-hoc scattering communication networks," in *2019 IEEE International Conference on Communications Workshops*. IEEE, 2019.